International Journal of
Molecular Sciences

MDPI

Article

Development of Novel Pt(IV)-Carbohydrate Derivatives as Targeted Anticancer Agents against Osteosarcoma

Eoin Moynihan [1], Silvia Panseri [2], Giada Bassi [2,3], Arianna Rossi [2,4], Elisabetta Campodoni [2], Eithne Dempsey [1,5], Monica Montesi [2,*], Trinidad Velasco-Torrijos [1,5] and Diego Montagner [1,5,*]

1 Department of Chemistry, Maynooth University, W23 F2H6 Maynooth, Ireland
2 Institute of Science, Technology and Sustainability for Ceramics, National Research Council (CNR), 48018 Faenza, Italy
3 Department of Neuroscience, Imaging and Clinical Sciences, University of Studies "G. D'Annunzio", 66100 Chieti, Italy
4 Department of Chemical, Biological, Pharmaceutical and Environmental Sciences, University of Messina, 98166 Messina, Italy
5 Kathleen Londsdale Institute for Human Health Research, Maynooth University, W23 F2H6 Maynooth, Ireland
* Correspondence: monica.montesi@issmc.cnr.it (M.M.); diego.montagner@mu.ie (D.M.)

Abstract: Despite the enormous importance of cisplatin as a chemotherapeutic agent, its application is impacted by dose-limiting side effects and lack of selectivity for cancer cells. Researchers can overcome these issues by taking advantage of the pro-drug nature of the platinum(IV) oxidation state, and by modifying the coordination sphere of the metal centre with specific vectors whose receptors are overexpressed in tumour cell membranes (e.g., carbohydrates). In this paper we report the synthesis of four novel carbohydrate-modified Pt(IV) pro-drugs, based on the cisplatin scaffold, and their biological activity against osteosarcoma (OS), a malignant tumour which is most common in adolescents and young adults. The carbohydrate-targeting vectors and Pt scaffold are linked using copper-catalysed azide–alkyne cycloaddition (CuAAC) chemistry, which is synonymous with mild and robust reaction conditions. The novel complexes are characterised using multinuclear 1D-2D NMR (^{1}H, ^{13}C and ^{195}Pt), IR, HR-MS, Elem. Analyses, and CV. Cytotoxicity on 2D and 3D and cell morphology studies on OS cell lines, as well as non-cancerous human foetal osteoblasts (hFOBs), are discussed.

Keywords: Pt(IV) pro-drugs; cisplatin; carbohydrate; selective targeting; osteosarcoma; healthy cell; click chemistry

Citation: Moynihan, E.; Panseri, S.; Bassi, G.; Rossi, A.; Campodoni, E.; Dempsey, E.; Montesi, M.; Velasco-Torrijos, T.; Montagner, D. Development of Novel Pt(IV)-Carbohydrate Derivatives as Targeted Anticancer Agents against Osteosarcoma. *Int. J. Mol. Sci.* **2023**, *24*, 6028. https://doi.org/10.3390/ijms24076028

Academic Editors: Marialuisa Piccolo and Claudia Riccardi

Received: 27 February 2023
Revised: 14 March 2023
Accepted: 17 March 2023
Published: 23 March 2023

1. Introduction

Cisplatin has been one of the most commonly used Platinum(II) chemotherapeutic drugs since its approval for clinical use over 40 years ago. However, issues associated with acquired or innate resistance, as well as dose-limiting side effects, have stymied its therapeutic potential [1]. Second and third generation Pt(II)-based chemotherapeutics, carboplatin and oxaliplatin, are used to combat resistance, by lowering hydration rates in the case of carboplatin, and by a different mechanism of action that avoids cross-resistance with cisplatin in the case of oxaliplatin [2]. While these drugs have helped to alleviate cisplatin resistance in a variety of cancers, the main problem is still a lack of targeted therapy to reduce the severe side effects associated with platinum-based drugs [3]. Platinum(IV) complexes have the potential to overcome some of the drawbacks of currently available Pt(II) drugs. They are more kinetically inert in comparison to their Pt(II) counterparts, which results in lower toxic side effects for the patient. These complexes are referred to as pro-drugs as they must be reduced from the inactive Pt(IV) complex to their active Pt(II) species by the reducing environment within cancer cells, which leads to a more

targeted approach of drug delivery to the cancer cells [4]. The most promising Pt(IV) drugs are satraplatin [5,6], ormaplatin [7,8] and iproplatin [9,10] but, despite promising results, none to date have been approved for widespread use in cancer treatments (Figure 1a) [3]. Promising strategies for imparting selectivity to Pt(IV) pro-drugs is the use of tumour-targeting ligands. Carbohydrates, such as glucose and galactose, can be used to exploit the Warburg effect [11], because cancer cells metabolise glucose differently from healthy cells. Rapid proliferation of cancer cells leads to the imbalance in the intake of oxygen and results in hypoxia, which drives cancer cells to choose anaerobic glycolysis to produce energy. This method of energy production is inefficient and leads to the overexpression of glucose transporters (GLUTs) on the cell membrane [12]. Several glyco-modified Pt(IV) complexes have been reported in literature, mainly from the group of Wang and co-workers [13–17], summarised excellently by Kenny and Marmion [3]. The most notable results were obtained when the Pt scaffold was cisplatin rather than carboplatin or oxalilplatin [18]. It was also determined that mono-functionalisation was more effective than bis-functionalised complexes [14]. Platinum-based complexes are extensively used to treat osteosarcoma (OS), the most common malignant primary bone tumour which affects adolescents and young adults, with a second spike of incidence in those over 50, and which tends to metastasize and invade para-carcinoma tissues [19]. Currently, treatment options incorporate surgery and combination chemotherapy, which cures 70% of patients. However, for patients with metastatic or relapsed OS, the modes of treatment have remained unchanged for over 30 years and result in a significantly lower survival rate among patients [20]. This reduction in survivability is partially because cisplatin is a standard drug in the treatment of OS and has limited effectiveness, stemming from chemoresistance and a lack of drug selectivity. This lack of selectivity and a need to overcome cisplatin resistance has led many to develop novel compounds to target specific molecular alterations in tumours, with the objective of restoring chemosensitivity [21]. Recently, our group reported the synthesis and biological evaluation against osteosarcoma of four acetylated glyco-modified Pt(IV) complexes, but, despite the promising results, the role of the sugars was not completely clarified [22]. The glycosylated complexes proved to have an enhanced cellular uptake, but this was probably due to the higher lipophilicity caused by the acetylated groups, rather than due to recognition by GLUTs. Indeed, these protecting groups are prone to enzymatic hydrolysis in the body, ultimately making them pro-drugs themselves [23]. The crystal structures of various GLUTs have enabled researchers to focus their work on the optimal presentation of their carbohydrates to target these transporters [24,25], and free sugars are employed as they more closely mimic the structure of the compounds recognised by various GLUTs that are overexpressed on cancer cell membranes. To try to clarify this aspect, we decided to synthesise four glyco-derivatives (two with glucose and two with galactose) for the previously reported complexes with the deprotected (free) sugars and evaluate their biological activity against two osteosarcoma cell lines and a non-cancerous human foetal osteoblast (hFOB), (Figure 1b). In this work we functionalise our carbohydrate-targeting vector in β configuration at the anomeric position, since an important factor for maintaining recognition is to conserve the sugars' ability to form hydrogen bonds with the GLUT binding site through the atom bound to the anomeric position acting as a H-bond acceptor [26]. To maintain this H-bonding ability, we take advantage of the copper-catalysed azide–alkyne cycloaddition (CuAAC) reaction due to its versatile nature and mild reaction conditions for the conjugation of our carbohydrates to the platinum core. The resulting 1,2,3-Triazole is recognised as a strong bio-isostere for many functionalities, including amide bonds, and has H-bonding acceptor properties [27]. Additionally, we wanted to investigate the use of both an anomeric *O*-ethylene linker (which resembles naturally occurring glycosides) and *N*-triazolyl glycomimetics, to analyse if there is a significant difference in the H-bond acceptor ability, and subsequent activity, of either group (Figure 1b).

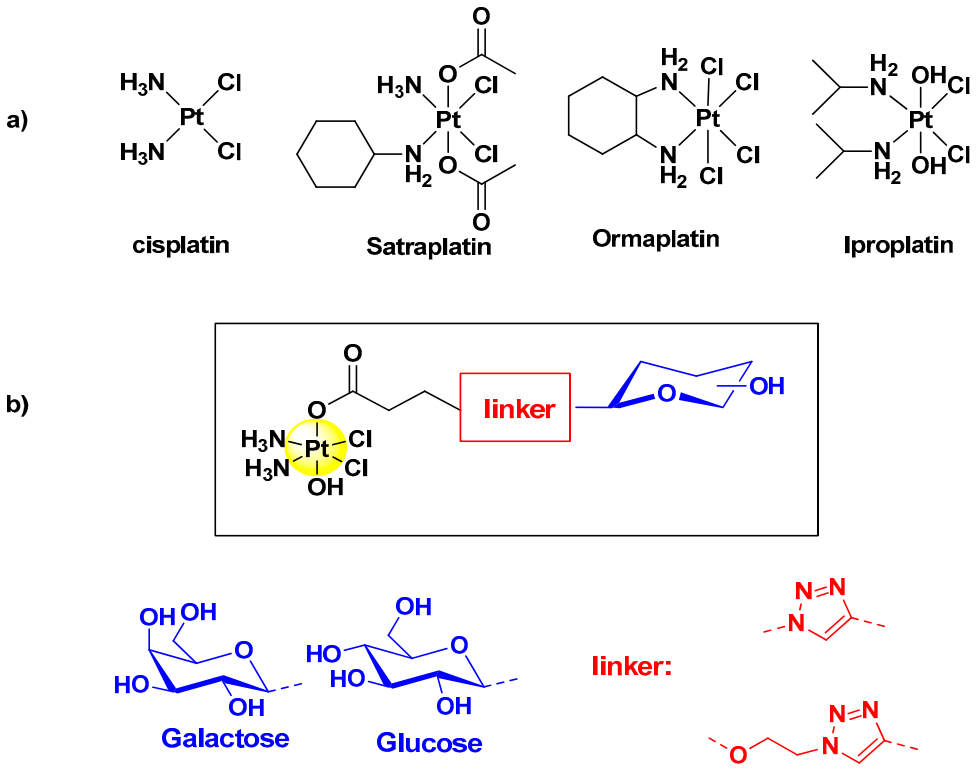

Figure 1. (**a**) Structures of cisplatin (*cis*-[$(NH_3)_2PtCl_2$]) and of the three most promising Pt(IV) complexes, satraplatin (*cis*,*trans*,*cis*-[$PtCl_2(OAc)_2(NH_3)$-cyclohexylamine]), ormaplatin ([$PtCl_4$(cyclohexane-1,2-diamine)]), and iproplatin (*cis*,*trans*,*cis*-[$PtCl_2(OH)_2$(isopropylamine)$_2$]). (**b**) General structure for the novel Pt(IV) complexes based on the cisplatin scaffold and functionalised with glucose and galactose.

The anticancer activity of the glyco-derivatives reported here have been investigated in both standard 2D and in 3D scaffold-based OS in vitro models, using two different OS cell lines (MG63 and SAOS-2) and osteoblast cells line (hFOBs) as healthy cells to compare the effectiveness against a standard of cisplatin.

2. Results and Discussion

2.1. Synthesis and Characterisation

As described in the introduction, the aim of this work is to synthesise Pt(IV) anticancer pro-drugs based on a cisplatin scaffold modified with free sugars (glucose and galactose) that could act as delivery vectors to enhance selectivity for cancer cells, exploiting the Warburg effect. With respect to our recent work [22], the sugars here are de-acetylated to obtain a more reliable recognition by the GLUT receptors overexpressed on the cancer cell membrane, as discussed in the introduction. The sugar moieties are connected to the platinum centre via a triazolyl linker exploiting the versatility and mild conditions of click chemistry copper azide–alkyne cycloaddition (CuAAC) reactions, producing four novel complexes. The synthesis of the novel glycosylated Pt(IV) complexes proved to be rather challenging; in fact, the direct deprotection of the corresponding acetylated glycosylated precursor complexes, recently reported by us [22], did not produce the expected results. The use of standard deprotection methods (i.e., NEt_3 in MeOH) resulted in the decomposition of the complexes, forming a series of impurities and a complex mixture which was very difficult to purify and isolate. After several attempts and modifications, the final complexes were successfully synthesised, as shown in Schemes 1 and 2.

Scheme 1 represents the synthetic mechanism route to produce the N-glycoside (glucose and galactose) derivatives with shorter chains. The synthesis of compounds **5**–**10** has been reported by us previously [22]. To summarise briefly, the per-acetylated glucose

5 and galactose **6** are transformed to the corresponding β-azides, **7** and **8**, through reaction with azidotrimethylsilane and tin tetrachloride. Following this, **7** and **8** are reacted with 4-pentynoic acid, using CuAAC conditions at room temperature, to produce the carboxylic acids **9** and **10**. At this point, the acetylated sugars are deprotected with triethylamine in a mixture of MeOH/H_2O at 45 °C to yield carboxylic acids **11** and **12**. Many standard coupling reagents and conditions were screened in order to identify a suitable procedure that would allow for the synthesis of activated N-hydroxysuccinimide (NHS) esters **13** and **14** in the presence of the hydroxyl groups in the deprotected sugars. Initial attempts for the classic activation with NHS using EDCI or TBTU did not yield the desired products. Finally, optimised reaction conditions with TSTU (N,N,N′,N′-Tetramethyl-O-(N-succinimidyl)uronium tetrafluoroborate) produced the activated NHS-esters **13** and **14** with good yield and purity. The advantage of using TSTU is that the reaction does not require the use of an additional coupling reagent and vastly reduces reaction time to a mere 20 min. The final complexes **1** and **2** were obtained through the dropwise addition of **13** and **14** to oxoplatin in DMSO over 2 days. The final complexes were characterised using ^{1}H, ^{13}C, ^{195}Pt-NMR, mass spectroscopy and cyclic voltammetry, and the purity was assessed with El. Anal. And HPLC (See Experimental Section and Supporting Information).

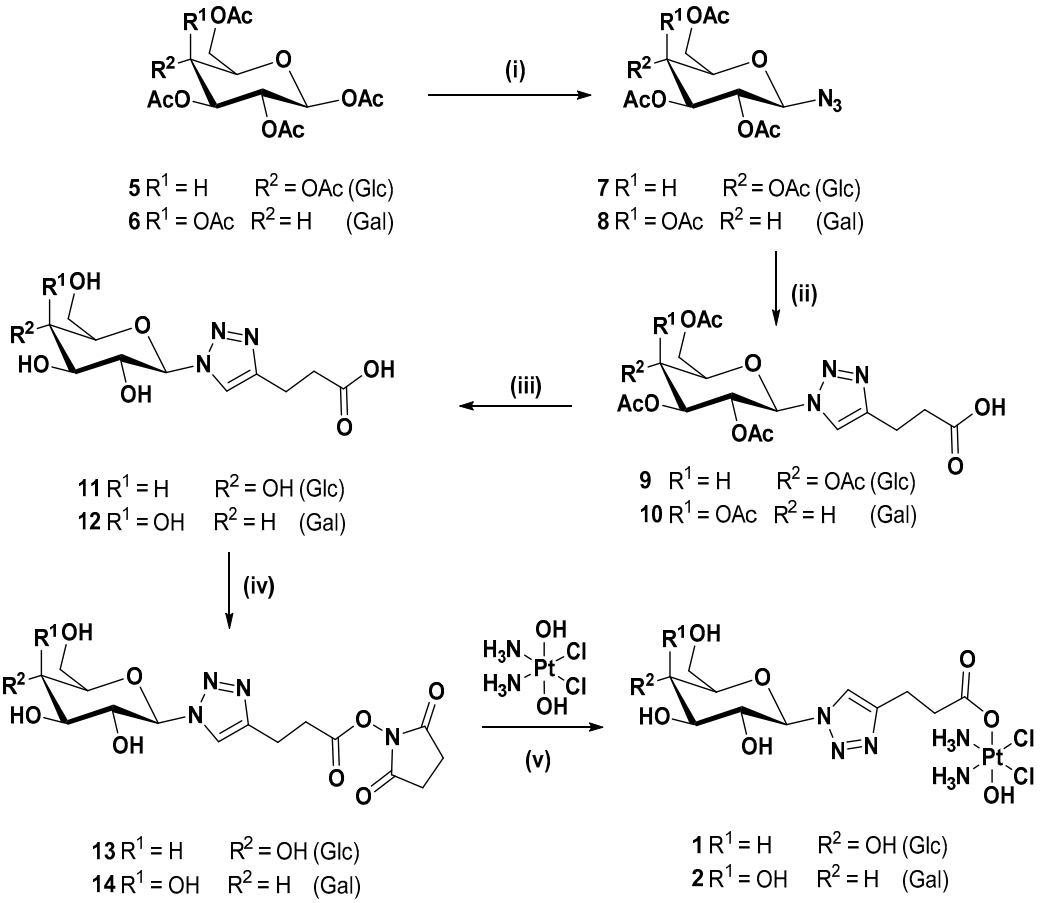

Scheme 1. Synthetic route for the complexes **1** and **2**: (i) $TMSN_3$, $SnCl_4$, DCM, rt, 16 h, 91% (**7**), 89% (**8**); (ii) 4-pentynoic acid, $CuSO_4$, sodium ascorbate, t-BuOH, THF, H_2O, rt, 16 h, 64% (**9**), 74% (**10**); (iii) TEA, MeOH, H_2O, 45 °C, 16 h, 95% (**11**), 97% (**12**); (iv) TSTU, TEA, DMF, rt, 20 min, 68% (**13**), 68% (**14**); (v) DMSO, 40 °C, 48 h, 59% (**1**), 35% (**2**).

Complexes **3** and **4,** with a O-ethylene linker, were synthesised according to Scheme 2, in a manner similar to the synthesis of the N-triazolyl derivatives **1** and **2,** described earlier. Compounds **19** and **20**, recently reported by us [22], were hydrolysed under mild basic conditions to afford deacetylated carboxylic acids **21** and **22**. The same challenges

described above remained for the synthesis of free sugar complexes **3** and **4** and consequently, the same strategies were applied. The successful formation of the NHS active esters **23** and **24** was achieved once again with the use of TSTU, and the final complexes **3** and **4** were obtained through the reaction of the activated deprotected sugar moieties **23** and **24** with oxoplatin in DMSO. These complexes were characterised using the same techniques as for complexes **1** and **2**. All the complexes show the typical features of Pt(IV) species based on a cisplatin scaffold, with a broad triplet around 6 ppm assigned to the NH_3 groups in the ^{1}H-NMR spectrum, the ^{195}Pt signal around 1600 ppm, typical of Pt in the oxidation state +4 and the typical Pt isotopic pattern in the mass spectra (Supplementary Materials Figures S1–S16).

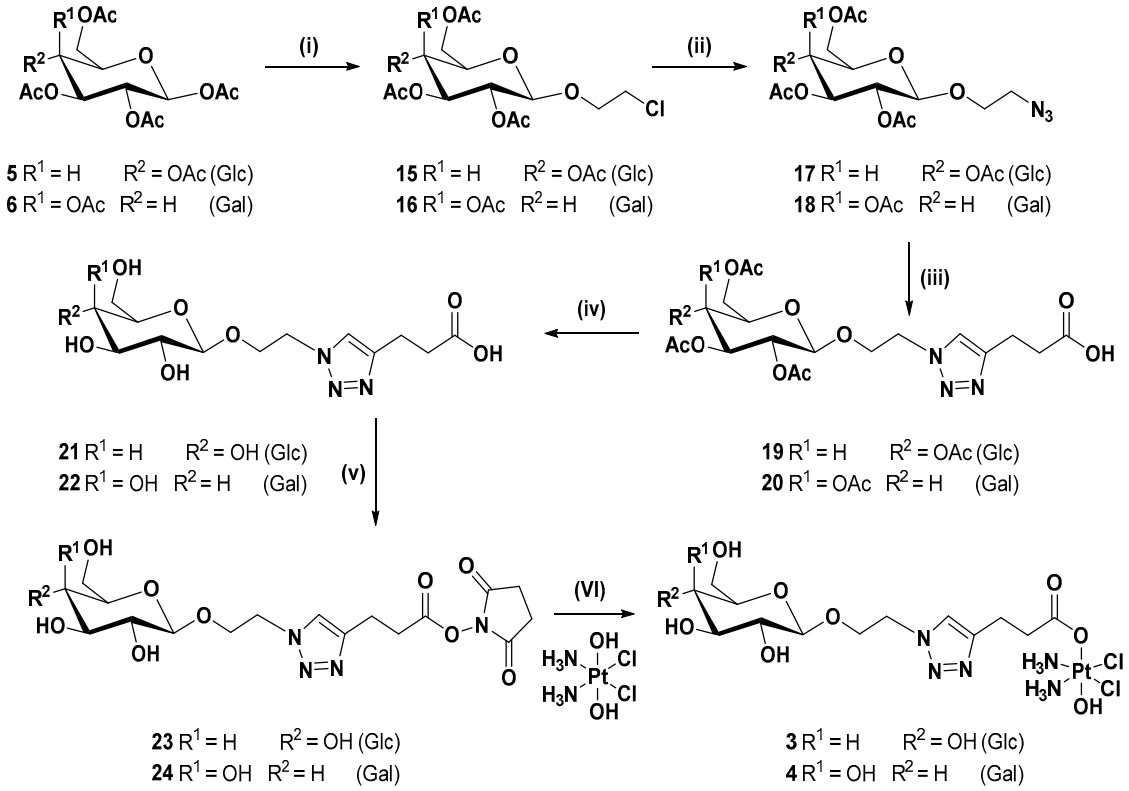

Scheme 2. Synthetic route for complexes **3** and **4**: (i) 2-Chloroethanol, BF_3.OEt_2, 3 Å MS, 0 °C to rt, DCM, 16 h, 39% (**15**), 40% (**16**); (ii) NaN_3, DMF, 80 °C, 16 h, 59% (**17**), 57% (**18**); (iii) $CuSO_4$, sodium ascorbate, t-BuOH, THF, H_2O, rt, 16 h, 44% (**19**), 47% (**20**); (iv) TEA, MeOH, H_2O, 45 °C, 16 h, 86% (**21**), 96% (**22**); (v) TSTU, TEA, DMF, 20 min, rt, 60% (**23**), 75% (**24**); (vi) DMSO, 40 °C, 48 h, 47% (**3**), 61% (**4**).

The stability in physiological conditions of complexes **1** and **3**, taken as examples for the different substituents at the anomeric position) was analysed over a period of 96 h via ^{1}H, ^{13}C and ^{195}Pt-NMR in a solution of DMSO containing PBS buffer (pH = 6.8) and minimum decomposition was observed (Figure S17a–f in Supplementary Materials). The redox behaviour of complexes **1** and **3** (cathodic processes E_p^c (I), E_p^c (II), Figure 2) and of the corresponding axial glycol-ligands **11** and **21** (E_p^c (I), Figure 2) was studied via Cyclic Voltammetry with $E^0_{Pt(IV)/Pt(II)}$ = −1.034 V and −1.002 V for **1** and **3,** respectively E_p^c (II). The electrochemical reduction was irreversible, in line with previous reported Pt(IV) species based on cisplatin [28], and no major difference was observed according to the type of linker used to connect the carbohydrate moiety and the Pt centre (Figure 2, Figures S18 and S19 in Supplementary Materials).

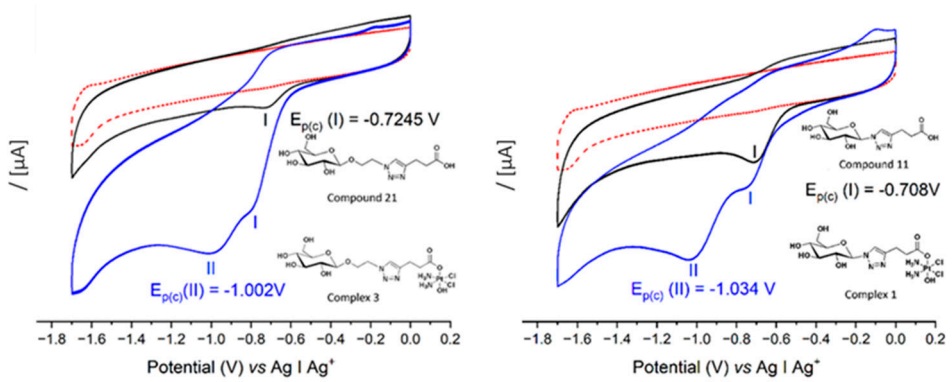

Figure 2. The cyclic voltammograms of the complexes **1** and **3** (blue), with evidence of irreversible cathodic processes I and II and of the axial ligands **11** and **21** (black), showing process I only, with background supporting electrolyte (red). All experiments were performed at the same concentration ([compound] = 2 mM) in deuterated 0.1 M DMSO-[*n*-Bu_4N][PF_6] at a scan rate of 0.1 Vs^{-1}.

For a confirmation of the activation through intracellular reduction that occurs in Pt(IV) species, the behaviour of the Pt(IV) pro-drugs was studied by means of the addition of an excess of ascorbic acid into a solution of complex **3** [29]. The reduction process was followed by ^{1}H-NMR with complete release of the carbohydrate axial ligand after 48 h, as observed by the disappearance of the triazole proton at δ = 7.93 of complex **3** and the concomitant formation of the corresponding peak at δ = 7.91 of the free carboxylic acid **21** (Figure 3 and Figure S20 in Supplementary Materials).

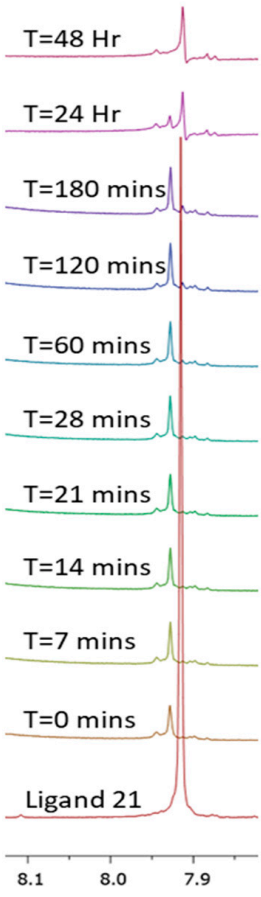

Figure 3. Reduction of complex **3** by a 10-fold excess of ascorbic acid. ^{1}H NMR spectra over 48 h in DMSO.

2.2. Biological Evaluation

The anticancer activity of the four complexes were tested in vitro in 2D and 3D against two osteosarcoma cancer cell lines (SAOS and MG63) and also in 2D against a healthy osteoblast cell line (hFOBs), to evaluate if the strategic use of glucose and galactose as vectors is enhancing the selectivity.

The evaluation of cell viability demonstrated a dose-dependent cancer cell toxicity exerted by all the drugs (Figure 4). Although no significant differences in the IC_{50} (Table 1, Figures S21–S23 in Supplementary Materials) were detected in the four complexes compared to cisplatin, at high concentrations the complexes showed better performance with respect to cisplatin. In MG63 cells, the mean effect of the complexes **1–4** showed a ~3-fold reduction of the cell viability with respect to cisplatin, and ~1.5-fold reduction for SAOS-2 (Figure 4). The higher anticancer activity of all the complexes **1–4,** with respect to cisplatin, was statistically significant at 30 μM for SAOS-2 and 60 μM for MG63. The different cellular behaviour between the cell lines can be attributed to the intrinsic biological differences of the two osteosarcoma cell lines [30].

Most importantly, in the healthy cell hFOBs, the cisplatin began to be extremely toxic at very low concentration, 1.5 μM ($p \leq 0.001$ with respect to cells only), while complexes **1–4** showed a cytotoxic effect at much higher concentrations, ≥ 15 μM (complex 1 $p \leq 0.05$; 2 $p \leq 0.001$; 3 $p \leq 0.0001$; 4 $p \leq 0.001$ respect to cells only). The evaluation of the IC_{50} values confirmed the cell viability results; in fact, in the hFOBs, the IC_{50} of the cisplatin (i.e., 4.1 μM) was far lower compared to the IC_{50} values of complexes **1–4,** which were > 16 μM (Table 1). Moreover, it was shown that the toxic effect of the complexes is statistically significantly lower, with respect to the effect of cisplatin, at 1.5 μM, 5 μM, 15 μM, and 30 μM (Figure 4). The cell behaviours observed in the cell viability assay were also confirmed using morphological analysis, where a reduction in cell density directly related to the increase in drug concentration was detected (Figure S24 in Supplementary Materials).

The results demonstrated that complexes **1–4** all have selectivity for these cancer cells and a lower toxic effect on healthy hFOBs. We believe that this selectivity could be ascribable to the overexpression of the GLUT family members, specifically GLUT-1, observed in cancer cells leading to an increased glycolytic activity [31,32]. The higher toxicity of all complexes with respect to the cisplatin, observed in both MG63 and SAOS-2 at 30 μM and 60 μM, strengthens the hypothesis of the role of the GLUT receptor overexpression in the uptake, induced by the presence of sugar moieties connected to the drug, and consequently in the increased anticancer effect.

In order to confirm these promising results, a proof of concept in vitro was performed using more relevant cancer models. In fact, it is well known that the use of conventional 2D approaches show some limitations because they fail to mimic a real tumour's complexity, leading to a low predictivity of preclinical results [33,34]. To overcome this limitation, and to strengthen the results obtained in the previous 2D study, an MG63 cell line was cultured on a 3D scaffold that mimics the feature of the bone extracellular matrix (Figure 5C) from a physical, chemical, and nanostructural point of view, as previously demonstrated [35,36].

After the seeding of the MG63 cell line, the cells were able to interact and colonise the scaffold, providing a more mimetic 3D scaffold-based osteosarcoma model (3D OS model) which was then used to test the effect of the proposed drugs. As shown in Figure 5A,B, MG63 cells easily adhered to the nanostructure of the biomimetic scaffolds and, 48 h after seeding, the scaffolds were nearly completely covered by the cells, exhibiting their characteristic morphology and a high level of cell/material interactions.

It is well known that the behaviour of the cells cultured in 3D condition is different respect to the standard 2D model [37]. For this reason, before testing the complexes in the 3D OS mode, a preliminary evaluation of the cisplatin effective concentration was performed by comparing the toxicity of cisplatin 15 μM in 2D and in the 3D OS model. As shown in Figure S25 in Supplementary Materials, 15 μM of cisplatin did not compromise the cell viability in 3D OS model, though it significantly reduced the viable cells grown in 2D standard culture conditions (p-value ≤ 0.0001).

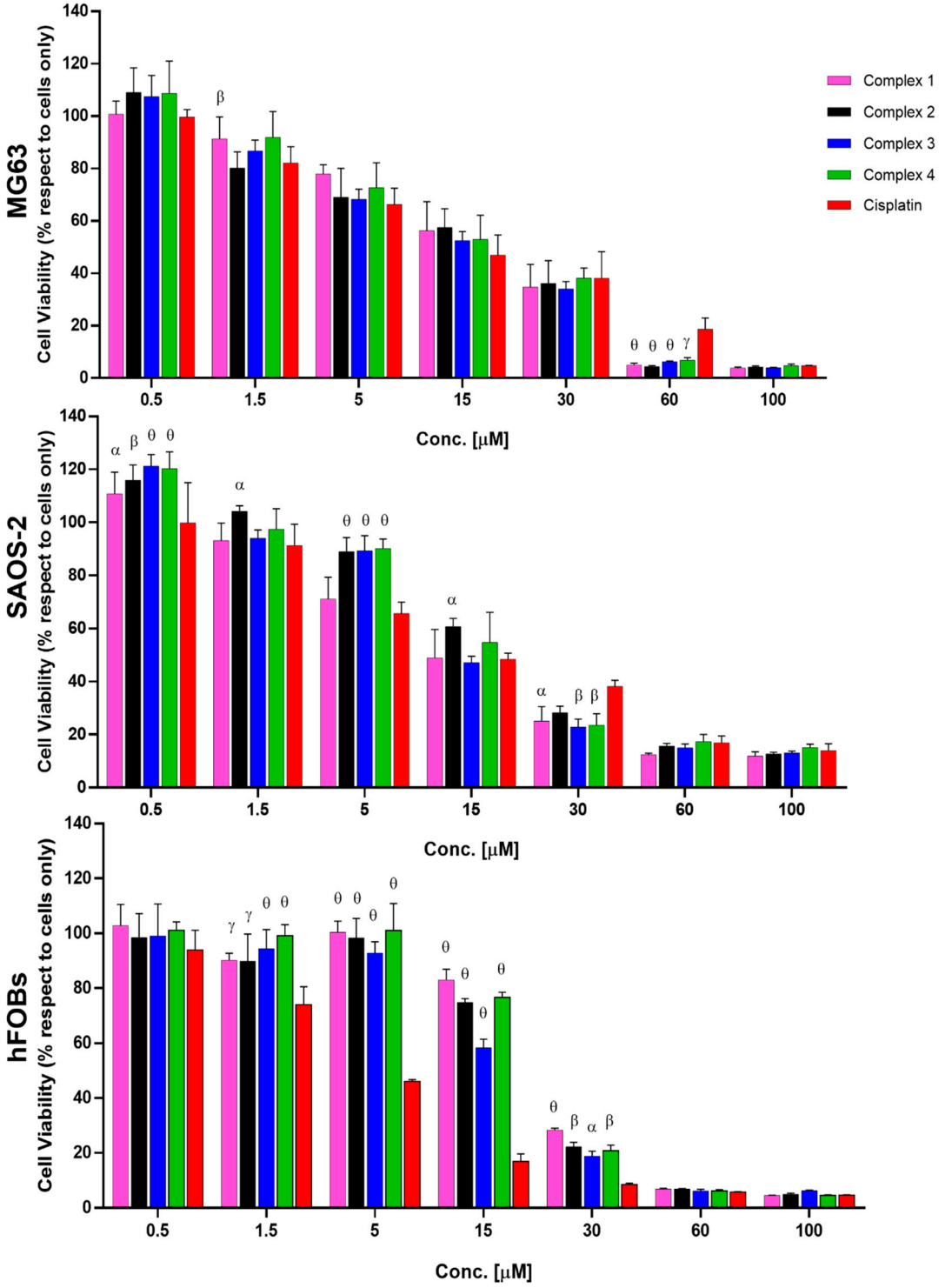

Figure 4. 2D drug screening of complexes **1–4** by MTT assay. Cell viability evaluation after 72 h incubation with complexes. Data are reported in the graph as percentage (%) mean ± standard error of the mean. Statistical analyses with respect to cisplatin are reported in the graph, p value is $\alpha \leq 0.05$, $\beta \leq 0.01$, $\gamma \leq 0.001$ and $\theta \leq 0.0001$.

Table 1. IC_{50} (μM) values of the complexes **1–4** and cisplatin against MG63, SAOS-2 and hFOBs cells.

	Cisplatin		Complex 1		Complex 2		Complex 3		Complex 4	
	IC_{50}	95% CI	IC_{50}	95% CI	IC_{50}	95% CI	IC_{50}	95% CI	IC_{50}	95% CI
MG63	12.20	+3.1; −2.6	15.90	+3.3; −2.9	13.60	+5.2; −4.0	13.0	+3.2; −2.7	14.90	+4.2; −3.5
SAOS-2	13.70	+3.2; −2.7	12.94	+3.4; −3.0	19.09	+3.4; −3.0	15.18	+3.7; −3.1	17.22	+4.5; −3.7
hFOBs	4.109	+0.42; −0.47	23.36	+1.72; −1.82	20.85	+1.92; −2.11	16.88	+1.7; −1.75	20.91	+0.42; −0.47

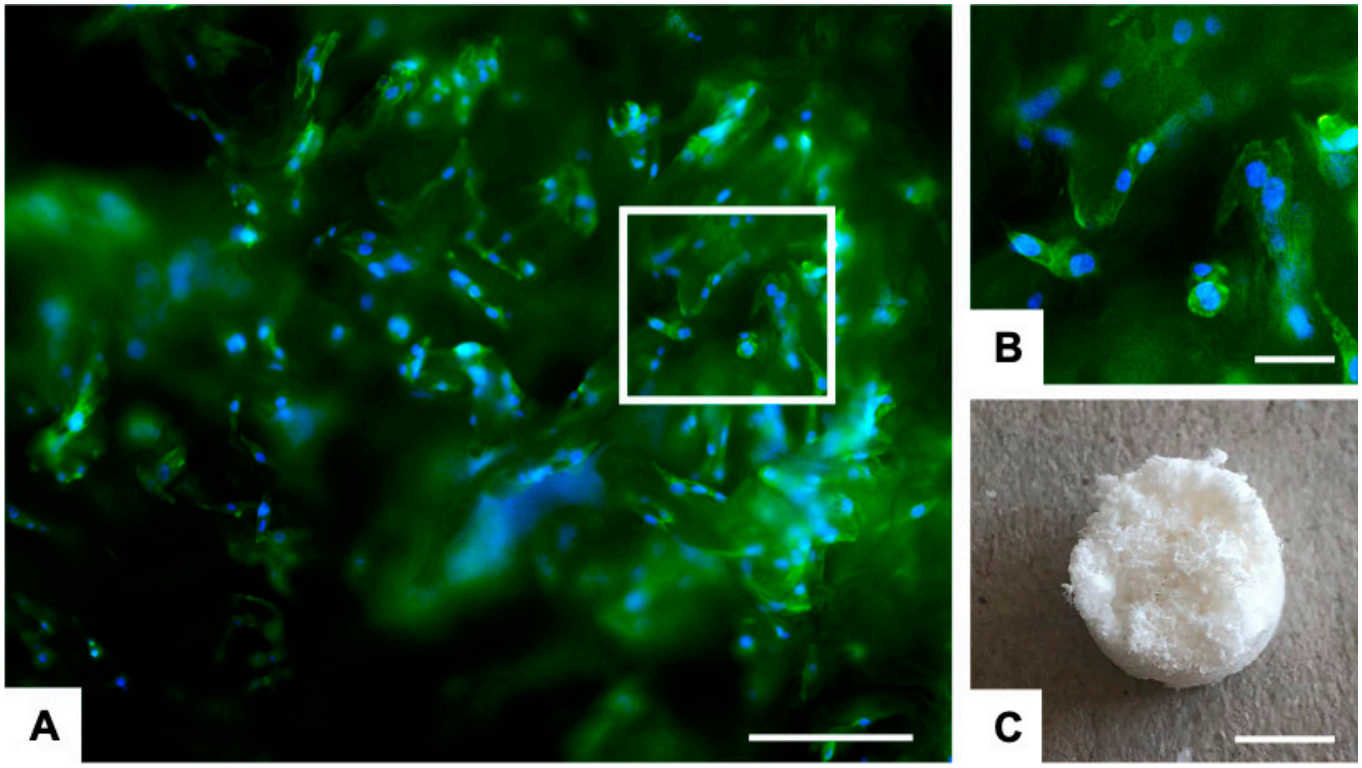

Figure 5. 3D scaffold-based osteosarcoma model (3D OS model). (**A**) Analysis of cell morphology of 3D MG63 culture on bone-mimetic scaffold 48 h after seeding. F-Actin filaments in green (FITC) and cell nuclei in blue (DAPI); scale bars 200 μm. (**B**) Image enlargement (white square) of the cell morphology details; scale bars 50 μm. (**C**) Representative image of the 3D bone-mimetic scaffold; scale bars 4 mm.

Based on these results, the complexes **1–4** and the cisplatin were tested at 30 and 60 μM in the 3D tumour model. At 60 μM, all the complexes showed higher toxic effect respect to the cisplatin, and these differences are statistically significant for complexes **2** and **4** with p value ≤ 0.05 (Figure 6). Morphological analysis (Figure S26 in Supplementary Materials) confirms the cell viability results.

This proof of concept highlights the cancer cells selectivity of the complexes for the considered OS cells, compared to the cisplatin action, and reinforces the data obtained in the 2D in vitro study, demonstrating better performances of the complexes **1–4** as anticancer drugs.

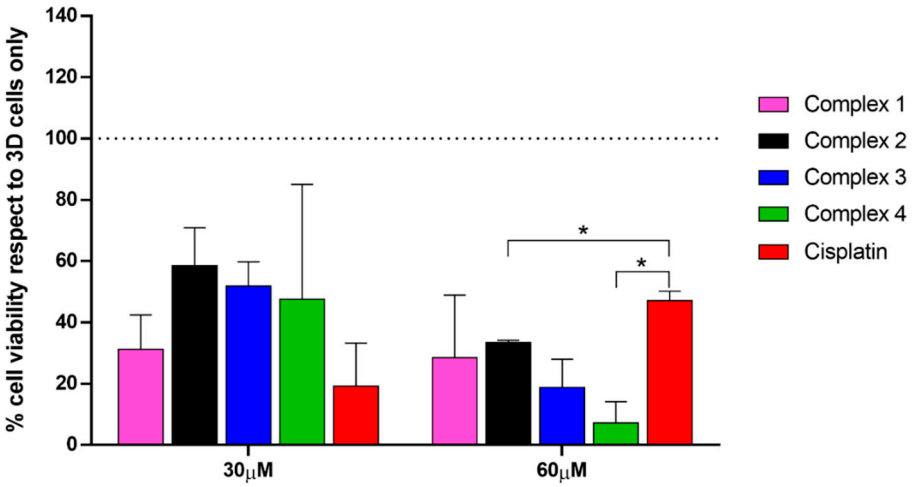

Figure 6. Anti-cancerous effect of **1–4** complexes on 3D OS model**.** Cell viability evaluation after 72 h of incubation with complexes using MTT assay. Data are reported in the graph as percentage (%) mean ± standard error of the mean. Statistical analyses with respect to cisplatin are reported in the graph, * p value ≤ 0.05.

3. Materials and Methods

3.1. General Methods

All reagents and reactants were purchased from commercial sources. The two sources used were Sigma-Aldrich (St.Louis, MO, USA) and Fluorochem (Graphite way, Hadfield, UK). All solvents were used without further purification. Cisplatin and oxoplatin were synthesised as previously reported [38,39]. Compounds **7–10** and **15–20** were synthesised as reported by us [22].

The elemental analysis studies (carbon, hydrogen, and nitrogen) were performed by means of a PerkinElmer 2400 series II analyser (Waltham, MA, USA). HR mass spectra were recorded with a Waters LCT Premier XE Spectrometer (Milford, MA, USA). NMR: ^{1}H, ^{13}C and ^{195}Pt NMR spectra were obtained in a solution of D_2O or DMSO-d_6 at 300 K, in 5 mm sample tubes, with a premium shielded Agilent Varian 500 MHz (operating at 500.13, 125.75, and 107.49 MHz, respectively)(Santa Clara, CA, USA). The ^{1}H and ^{13}C chemical shift was referenced to the residual impurity of the solvent. The external reference was Na_2PtCl_4 in D_2O (adjusted to $\delta = -1628$ ppm from Na_2PtCl_6) for ^{195}Pt. The stability was followed using high-performance liquid chromatography (HPLC) with a Phenomenex Luna C18 (5 μM, 100 Å, 250 mm × 4.60 mm i.d.) column (Torrance, CA, USA) at room temperature at a flow rate of 1.0 mL/min with 254 nm UV detection. Mobile phase containing 80:20 acetonitrile (0.1% trifluoroacetic acid): water (0.1% trifluoroacetic acid): the complexes were dissolved in DMF (0.5 mL) and diluted to a final concentration of 0.5 mM, using acetonitrile and water solution (1/1) and 2 mM 4-(2-hydroxyethyl)piperazine-1-ethanesulfonic acid (HEPES) buffer (pH 6.8). Infrared (IR) spectra were precisely recorded in the region 4000–400 cm^{-1} on a Perkin Elmer spectrum 100 FT/IR spectrometer (Shelton, CT, USA). The solid samples were run using ATR. An extensive biological evaluation of the activity of all the compounds was performed in human osteosarcoma cell line in vitro models as reported below.

3.2. Cyclic Voltammetry

Measurements were made using a Solartron SI2187 Electrochemical Potentiostat/Galvanostat (Berwyn, PA, USA) and a CHI Instruments 1200 Potentiostat (Austin, TX, USA). Non-aqueous voltammetry of 2 mM of each of **11**, **21**, **1** and **3** was carried out at a glassy carbon working electrode (0.07 cm^2) in a three-electrode configuration with Pt wire counter and non-aqueous $Ag|Ag^+$ reference electrode in 0.1 M tetrabutylammonium hexafluorophosphate ($TBAPF_6$) supporting electrolyte in DMSO as solvent. The working electrodes were prepared by polishing with 1 μm microcrystalline diamond suspension on a micro-cloth,

followed by rinsing in deionised water. Voltammograms were generated over the range 0.2 to −1.7 V vs. Ag/Ag^+ in a deaerated solution (N_2 bubbling 10 min), with a cathodic scan direction at 100 $mV \cdot s^{-1}$ in all cases.

3.3. Stability and Reduction Studies

The stability was analysed via ^1H, ^{13}C and ^{195}Pt NMR. Complexes **1** and **3** (taken as examples for the different substituents at the anomeric position) were dissolved in a 1/1 mixture of DMSO and PBS (pH = 6.8), and the spectra were collected after 0 and 96 h. The reduction was followed by ^1H-NMR. Complex 3 (5 mg, 7.53 μmol) was dissolved in 500 μL of DMSO-d_6 and ascorbic acid (13 mg, 10 Equiv.) was added. ^1H NMR spectrum was recorded every 7 min for 30 min, then every hour until 24 h and then after 48 h.

3.4. In Vitro Biological Evaluation

In vitro tests of the four Pt(IV)-Carbohydrate derivatives complexes (**1**–**4**) were performed to evaluate their biological activity towards two osteosarcoma cell lines (MG63 and SAOS-2) and a non-cancerous cell line of human foetal osteoblasts (hFOBs), compared to cisplatin. The drugs were reconstituted in dimethyl sulfoxide (DMSO) at 1 mg/mL concentration, before being diluted in culture media at the required concentration. A 2D in vitro screening of all the drugs was performed at 72 h in a wide concentration range (0.5; 1.5, 5, 15, 30, 60 and 100 μM) on the three different cell lines in terms of cell viability, and the IC_{50} was calculated. The cell morphology in the presence of the complexes was evaluated at 15 and 30 μM concentrations, for MG63 and SAOS-2 and hFOBs cells, respectively, according to the IC_{50} at 72 h. Moreover, as more predictive in vitro cell culture systems, 3D tumour scaffold-based models of osteosarcoma were developed, and the anticancer activity of cisplatin and complexes **1**–**4** on MG63 cells, in terms of cell viability and morphology, was investigated at 30 and 60 μM concentrations after 72 h of culture. For the models, a composite hydroxyapatite-based scaffold (MgHA/Coll), as a bone-like matrix, was used in combination with MG63 cells. For both the 2D and 3D in vitro cell cultures, cisplatin was used as a control group, and cells only were used as a negative control.

Cell culture. Human Osteosarcoma cell lines MG63 (ATCC® CRL1427™), SAOS-2 (ATCC® HTB-85™), and Human Foetal Osteoblasts (hFOBs 1.19) (ATCC® CRL-11372™) were purchased from American Type Culture Collection (ATCC) and used for this study. The MG63 cell line was cultured in DMEM F12-GlutaMAX™ Modified Medium (Gibco), supplemented with 10% Foetal Bovine Serum (FBS) (Gibco) and 1% of penicillin/streptomycin mixture (pen/strep) (100 U/mL–100 μg/mL, Gibco). The SAOS-2 cell line was cultured in McCoy's 5A Modified Medium (Gibco), supplemented with 15% and 10% FBS, respectively, and 1% pen/strep. The hFOBs cell line was cultured in DMEM F12 no phenol red, with L-glutamine supplemented with 10% FBS and 0.3 mg/mL Geneticin (G418, Gibco). Cells were kept in an incubator at 37 °C under controlled humidity and 5% CO_2 atmosphere conditions. Cells were detached from culture flasks via trypsinization and centrifuged. The cell number and viability were determined using the trypan blue dye exclusion test, and all cell handling procedures were performed under a laminar flow hood in sterility conditions.

Synthesis of bone-mimetic scaffolds. The Mg-doped hydroxyapatite collagen composite scaffolds were designed and synthesised at ISSMC of CNR of Italy [35]. In brief, 150 g of collagen gel (1 wt%, Opocrin SpA, MO, Italy) was diluted into a phosphoric acid solution (2.4 g in 500 mL; H_3PO_4, 85 wt.%, Sigma-Aldrich) at room temperature to obtain an acidic aqueous homogenous suspension. Separately, a basic aqueous suspension was obtained by mixing 2.7 g of calcium hydroxide ($Ca(OH)_2$, 95 wt.%, Sigma) and 0.35 g of magnesium chloride ($MgCl_2 \cdot 6H_2O$, 99 wt.%, Sigma) in 500 mL of milli-Q water at room temperature to obtain a basic aqueous homogenous suspension. The acidic suspension was dripped into the basic one at 25 ± 2 °C under continuous stirring condition and maturated for 2 h. Later, the slurry solution was rinsed thrice in milli-Q water and filtered through metallic sieve (150 m) to exclude unreacted counter ions. The recovered slurry solution was cross-linked with 2 wt.% BDDGE (respect to Collagen) at 25 ± 2 °C for 24 h and at 4 °C for other

24 h. Later, the solution was rinsed thrice in milli-Q water to remove any residues and freeze-dried (−40 °C and +25 °C) for 48 h under 0.086 mbar vacuum conditions (LIO 3000 PLT, 5PASCAL, Italy). The obtained scaffolds (8 × 4 mm), named bone-mimetic scaffolds, were sterilised using 25 kGy γ-ray irradiation before use.

3D scaffold-based osteosarcoma models (3D OS model). For the development of the in vitro 3D scaffold-based osteosarcoma model, bone-mimetic scaffolds were used as bone-like matrix in combination with MG63 cells. The scaffolds were conditioned in culture media for 24 h before the cell seeding. MG63 cell line was seeded with a density of 3.0×10^4 per scaffold by dropping the cellular suspension on the material upper surface followed by 30 min pre-adhesion at 37 °C before cell media addition. The 3D OS model has been grown in the incubator under standard culture medium condition for 48 h to allow cell colonization of the scaffold, then the medium was changed, and the drugs were added. The in vitro 3D OS models were cultured in the presence of the drugs for 72 h at 37 °C under controlled humidity and 5% CO_2 atmosphere conditions; the cells grown in 3D in standard condition, without the drugs, were used as control group (3D cells only). All cell handling procedures were performed under a laminar flow hood in sterility conditions.

MTT cell viability assay. A quantitative analysis of cell viability was carried out by using MTT assay, following the manufacturer's instructions. For the in vitro 2D cell cultures, all cell lines were seeded at a density of 5.0×10^3 cells/well in 96 well-plates. For in vitro 3D cell cultures, see at the "3D scaffold-based models of osteosarcoma" paragraph of Materials and Methods section. The MTT reagent [3-(4,5-dimethylthiazol-2-yl)-2,5-diphenyltetrazolium bromide] (5 mg/mL) was dissolved in phosphate saline buffer 1X (PBS 1X). At 72 h, the cells were incubated with 10% media volume MTT solution for 2 h at 37 °C, 5% CO_2 and controlled humidity conditions. The cell culture media was removed and substituted with DMSO (Merck) dissolving formazan crystals, derived from MTT conversion by metabolically active cells. For the 3D scaffold-based models of osteosarcoma, each scaffold was transferred into a 2 mL Eppendorf, and completely broken using pestles after DMSO addition. After 15 min of incubation under slight stirring conditions, the absorbance of formazan was read at 570 nm by using a Multiskan FC Microplate Photometer (Thermo Fisher Scientific, Waltham, MA, USA). The values of absorbance are directly proportional to the number of metabolic active cells in each well. One experiment was carried out, and a biological triplicate for each condition was performed. For the 3D tumour models, one biological experiment was performed, and two scaffolds for each condition were used.

Cell morphology evaluation. For the in vitro 2D cell cultures, all cell lines were seeded at a density of 5.0×10^3 cells/well in 96 well-plates, for the in vitro 3D cell cultures cells were treated as previously described. Both the 2D and 3D cell cultures were fixed in 4% buffered Paraformaldehyde (PFA) following the manufacturer's instructions. The fixed samples were permeabilised in PBS 1X with 0.1% (v/v) Triton X-100 (Merck) for 5 min at room temperature and F-actin filaments were highlighted with Alexa Fluor 488 Phalloidin (Invitrogen) for 20 min at room temperature in the dark. DAPI (600 nM) counterstaining was performed for cell nuclei identification, following the manufacturer's instructions. The images were acquired by using an Inverted Ti-E Fluorescent Microscope.

Statistical Analysis. Statistical analysis was performed using GraphPad Prism Software (8.0.1 version). The results of the MTT assay of the in vitro 2D drug screening are reported in the graphs as mean percentage of cell viability, with respect to cells only ± standard deviation, and they were analysed using two-way analysis of variance (two-way ANOVA) and Dunnett's multiple comparisons test. The MTT results were further analysed using one-way analysis of variance (one-way ANOVA) and Dunnett's multiple comparisons test. IC_{50} values were calculated as Log(inhibitor) versus mean percentage of dead cells, with respect to cells only, and the obtained values are reported in the graphs ±95% confidence interval (CI) for each cell line. The MTT results for the 3D tumour engineered models of osteosarcoma were reported in the graph as percentage mean ± standard error of the mean, and they were analysed with two-way ANOVA and Dunnett's multiple comparisons test. A further analysis was performed using the unpaired *t*-test on all drugs, with respect to cisplatin.

3.5. Synthetic Procedures

Compounds **7–10** and **15–20** were synthesised as reported by us [22].

N-(β-D-glucopyranosyl-1,2,3-triazol-4-yl)-propanoic acid (11)

9 (0.612 g, 1.29 mmol) was suspended in a mixture of methanol (6 mL) and water (3 mL) and heated at 45 °C. NEt_3 (0.2 mL) was added, and the reaction was allowed to stir overnight. The progress was checked using TLC (95:5 DCM:MeOH). The solvent was removed under vacuum and the residue was redissolved in H_2O and stirred with Amberlite H^+ resin for 40 min. The Amberlite was filtered, and the residue was dried via lyophilization and reacted in the following step without further purification (0.375 g, 1.04 mmol, 95%). R_f = 0.40 (DCM:MeOH:H_2O 60:35:5). $[\alpha]_D^{21.4}$+1.12 (c 0.825, MeOH). ^{1}H NMR (500 MHz, D_2O) δ 7.97 (s, 1H, triaz-C*H*), 5.67 (d, *J* = 9.2 Hz, 1H, H-1), 3.95 (t, *J* = 9.2 Hz, 1H, H-2), 3.87 (dd, *J* = 12.4, 2.0 Hz, 1H, H-6), 3.77–3.64 (m, 3H, H-3, H-6′, H-5), 3.62–3.56 (m, 1H, H-4), 2.96 (t, *J* = 7.4 Hz, 2H, triaz-CH_2), 2.55 (t, *J* = 7.4 Hz, 2H, CH_2CO). ^{13}C NMR (125 MHz, D_2O) δ 180.90 (*C*O), 147.92 (triaz-*C*), 122.15 (triaz-CH), 87.35 (C-1), 78.79 (C-5), 75.87 (C-3), 72.22 (C-2), 68.92 (C-4), 60.40 (C-6), 36.18 (*C*H_2CO), 21.49 (triaz-*C*H_2). IR (ATR) 3256.84, 2915.58, 1567.38, 1396.39, 1042.54, 898.47, 599.49 cm^{-1}. HR-MS (+): *m*/*z* calcd for $C_{11}H_{17}N_3O_7$ + H^+ [M + H]$^+$ 304.1145, found 304.1140. HR-MS (+): *m*/*z* calcd for $C_{11}H_{17}N_3O_7$ + Na^+ [M + Na]$^+$ 326.0964, found 326.0958.

N-(β-D-glucopyranosyl-1,2,3-triazol-4-yl)-(3-oxopropyl-(oxy(2,5-dioxopyrrolidin-1-yl)))) (13)

11 (0.2 g, 0.659 mmol) was added to a flask containing TSTU (0.218 g, 0.725 mmol, 1.1 equiv.) and placed under N_2. Anhydrous DMF (10 mL) and anhydrous Triethylamine (0.101 mL, 0.725 mmol, 1.1 equiv.) were added. The reaction was stirred for 20 min, and reaction progress was monitored by TLC (60:35:5 DCM:MeOH:H_2O). The solvent was removed in vacuo and the residue was washed with DCM. The precipitate was collected via centrifugation and dried, yielding a light pink powder (Yield 0.182 g, 0.454 mmol, 68%). R_f = 0.92 (DCM:MeOH:H_2O 60:35:5). $[\alpha]_D^{23.5}$+ 3.75 (c 0.8, H_2O). ^{1}H NMR (500 MHz, DMSO) δ 8.11 (s, 1H, triaz-C*H*), 5.48 (d, *J* = 9.3 Hz, 1H, H-1), 5.32 (d, *J* = 6.0 Hz, 1H, O*H* of C-2), 5.26 (d, *J* = 4.6 Hz, 1H, O*H* of C-3), 5.14 (d, *J* = 5.4 Hz, 1H, O*H* of C-4), 4.62 (s, 1H,O*H* of C-6), 3.74–3.66 (m, 2H, H-2, H-6), 3.43 (d, *J* = 7.6 Hz, 2H, H-6′, H-5), 3.39 (dd, *J* = 8.9, 3.9 Hz, 1H, H-3), 3.21 (dt, *J* = 13.9, 7.0 Hz, 1H, H-4), 3.10–3.05 (m, 2H, CH_2CO), 3.02–2.98 (m, 2H, triaz-CH_2), 2.82 (s, 4H, CH_2CH_2-succ) ppm. ^{13}C NMR (125 MHz, DMSO) δ 170.25 (*C*O succ ×2), 168.38 (*C*O), 144.37 (triaz-*C*), 121.40 (triaz-*C*H), 87.44 (C-1), 79.92 (C-5), 76.95 (C-3), 72.16 (C-2), 69.60 (C-4), 60.74 (C-6), 29.58 (*C*H_2CO), 25.47 (*C*H_2CH_2-succ), 20.27 (triaz-*C*H_2) ppm. IR (ATR) 3298.62, 2917.68, 1731.73, 1708.88, 1406.06, 1367.70, 1206.78, 1019.20, 818.67, 647.68 cm^{-1}. HR-MS (+): *m*/*z* calcd for $C_{15}H_{20}N_4O_9$ + H^+ [M + H]$^+$ 401.1309, found 401.1300. HR-MS (+): *m*/*z* calcd for $C_{15}H_{20}N_4O_9$ + Na^+ [M + Na]$^+$ 423.1128, found 423.1119.

[Pt^{IV}(NH_3)$_2$(11)(OH)Cl_2] (1)

13 (0.321 g, 0.801 mmol) dissolved in DMSO (15 mL) was added dropwise overnight to a suspension of Oxoplatin (0.280 g, 0.841 mmol, 1.05 equiv.) in DMSO (5 mL) and stirred in the dark at 40 °C for 48 h. The yellow suspension was filtered and the DMSO was evaporated via lyophilization. The remaining oil was treated with methanol (10 mL) and the white/yellow precipitate that was formed was washed with DCM and diethyl ether. The product was dried under reduced pressure (Yield 0.293 g, 0.473 mmol, 59%). $[\alpha]_D^{22.5}$+2.22 (c 0.9, H_2O). ^{1}H NMR (500 MHz, DMSO) δ 8.06 (s, 1H, triaz-C*H*), 6.17–5.79 (m, 6H, 2x NH_3), 5.44 (d, *J* = 9.3 Hz, 1H, H-1), 5.32 (d, *J* = 6.0 Hz, 1H, O*H* of C-2), 5.27 (d, *J* = 4.8 Hz, 1H, O*H* of C-3), 5.14 (d, *J* = 5.4 Hz, 1H, O*H* of C-4), 4.63 (t, *J* = 5.6 Hz, 1H, O*H* of C-6), 3.77–3.65 (m, 2H, H-2, H-6), 3.43 (dt, *J* = 11.9, 4.9 Hz, 3H, H-6′, H-3, H-5), 3.21 (dd, *J* = 8.9, 5.2 Hz, 1H, H-4), 2.83 (t, *J* = 7.6 Hz, 2H, triaz-CH_2), 2.49 (m, 2H, CH_2CO). ^{13}C NMR (125 MHz, DMSO) δ 179.89 (*C*O), 146.33 (triaz-*C*), 121.23 (triaz-*C*H), 87.42 (C-1), 79.90 (C-5), 76.97 (C-3), 72.01 (C-2), 69.60 (C-4), 60.77 (C-6), 35.96 (CH_2CO), 21.93 (triaz-CH_2). ^{195}Pt{^{1}H} NMR (108 MHz, DMSO) δ 1047.07 ppm. IR (ATR) 3221.35, 1619.15, 1351.11, 1094.74, 579.32,

438.05 cm^{-1}. HR-MS (+): *m*/*z* calcd for $C_{11}H_{23}Cl_2N_5O_8Pt + H^+$ $[M + H]^+$ 619.0644, found 620.0639. El. Anal. Calcd. for $C_{11}H_{23}Cl_2N_5O_8Pt$: % C = 21.33; H = 3.74; N = 11.31; found: % C = 21.85; H = 3.39; N = 11.82.

***N*-(*β*-D-galactopyranosyl-1,2,3-triazol-4-yl)-propanoic acid (12)**

Compound **12** was synthesised according to the procedure reported for compound 11 (Yield 0.098 g, 0.323 mmol, 97%). R_f = 0.51 (DCM:MeOH:H_2O 60:35:5) $[\alpha]_D^{23.7}$+ 16 (c 0.625, MeOH). ^{1}H NMR (500 MHz, D_2O) δ 7.96 (s, 1H, triaz-C*H*), 5.55 (d, *J* = 9.2 Hz, 1H, H-1), 4.11 (t, *J* = 9.5 Hz, 1H, H-2), 3.99 (dd, *J* = 3.3, 0.7 Hz, 1H, H-4), 3.89 (td, *J* = 6.0, 0.8 Hz, 1H, H-5), 3.78 (dd, *J* = 9.8, 3.3 Hz, 1H, H-3), 3.69 (d, *J* = 6.2 Hz, 2H, H-6, H-6′), 2.89 (t, *J* = 7.4 Hz, 2H, triaz-CH_2), 2.52 (t, *J* = 7.4 Hz, 2H, CH_2CO). ^{13}C NMR (125 MHz, D_2O) δ 179.95 (*C*O), 147.63 (*C*-triaz), 121.90 (*C*H-triaz), 87.93 (C-1), 78.16 (C-5), 72.92 (C-3), 69.63 (C-2), 68.52 (C-4), 60.78 (C-6), 35.46 (*C*H_2CO), 21.20 (triaz-*C*H_2). IR (ATR) 3247.67, 1565.21, 1399.66, 1053.32, 883.22, 553.54 cm^{-1}. HR-MS (+): *m*/*z* calcd for $C_{11}H_{17}N_3O_7$ + H^+ $[M + H]^+$ 304.1145, found 304.1138. HR-MS (+): *m*/*z* calcd for $C_{11}H_{17}N_3O_7$ + Na^+ $[M + Na]^+$ 326.0964, found 326.0956.

***N*-(*β*-D-galactopyranosyl-1,2,3-triazol-4-yl)-(3-oxopropyl-(oxy(2,5-dioxopyrrolidin-1-yl))) (14)**

Compound **14** was prepared according to the method reported for compound 13 (Yield 0.204 g, 0.509 mmol, 68%). R_f = 0.9 (DCM:MeOH:H_2O 60:35:5). $[\alpha]_D^{23.5}$ − 4.28 (c 0.7, H_2O). ^{1}H NMR (500 MHz, DMSO) δ 8.07 (s, 1H, triaz-C*H*), 5.44 (d, *J* = 9.2 Hz, 1H, H-1), 5.16 (d, *J* = 6.0 Hz, 1H, O*H* of C-2), 5.03 (d, *J* = 5.7 Hz, 1H, O*H* of C-3), 4.70 (t, *J* = 5.7 Hz, 1H, O*H* of C-6), 4.66 (d, *J* = 4.9 Hz, 1H, O*H* of C-4), 4.03–3.96 (m, 1H, H-2), 3.76 (t, *J* = 3.75 Hz, 1H, H-4), 3.70 (t, *J* = 6.1 Hz, 1H, H-5), 3.56–3.44 (m, 3H, H-3, H-6, H-6′), 3.09 (t, *J* = 7.0 Hz, 2H, CH_2CO), 3.02–2.99 (m, 2H, triaz-CH_2), 2.82 (s, 2H, CH_2CH_2-succ). ^{13}C NMR (125 MHz, DMSO) δ 170.23 (*C*O succ ×2), 168.39 (*C*O), 144.42 (triaz-*C*), 121.12 (triaz-*C*H), 88.06 (C-1), 78.37 (C-5), 73.670 (C-3), 69.32 (C-2), 68.42 (C-4), 60.45 (C-6), 29.59 (*C*H_2CO), 25.46 (*C*H_2CH_2-succ), 20.28 (triaz-*C*H_2) ppm. IR (ATR) 3309.24, 2917.95, 1731.99, 1368.41, 1205.61, 1020.46, 891.00, 820.54, 647.48 cm^{-1}. HR-MS (+): *m*/*z* calcd for $C_{15}H_{20}N_4O_9 + H^+$ $[M + H]^+$ 401.1309, found 401.1305. HR-MS (+): *m*/*z* calcd for $C_{15}H_{20}N_4O_9 + Na^+$ $[M + Na]^+$ 423.1128, found 423.1127.

$[Pt^{IV}(NH_3)_2$(12)$(OH)Cl_2]$ (2)

Complex **2** was synthesised according to the method reported for complex 1 (Yield 0.111 g, 0.179 mmol, 35%). $[\alpha]_D^{23.5}$+ 10 (c 0.9, H_2O). ^{1}H NMR (500 MHz, DMSO) δ 8.00 (s, 1H, triaz-C*H*), 6.11–5.80 (br. t, 6H, 2x NH_3), 5.39 (d, *J* = 9.2 Hz, 1H, H-1), 5.18 (d, *J* = 5.9 Hz, 1H, O*H* of C-2), 5.03 (d, *J* = 5.6 Hz, 1H, O*H* of C-3), 4.70 (t, *J* = 5.6 Hz, 1H, O*H* of C-6), 4.64 (d, *J* = 5.1 Hz, 1H, O*H* of C-4), 4.05–3.98 (m, 1H, H-2), 3.75 (t, *J* = 3.6 Hz, 1H, H-4), 3.68 (t, *J* = 5.9 Hz, 1H, H-5), 3.56–3.47 (m, 3H, H-3, H-6, H-6′), 2.83 (t, *J* = 7.45 Hz, 2H, triaz-CH_2), 2.53–2.51 (m, 2H, CH_2CO, overlaps with DMSO). ^{13}C NMR (125 MHz, DMSO) δ 179.90 (*C*O), 146.35 (triaz-*C*), 120.97 (triaz-*C*H), 88.01 (C-1), 78.35 (C-5), 73.73 (C-3), 69.19 (C-2), 68.46 (C-4), 60.47 (C-6), 36.01 (*C*H_2CO), 21.94 (triaz-*C*H_2). ^{195}Pt{^{1}H} NMR (108 MHz, DMSO) δ 1045.09 ppm. IR (ATR) 3224.69, 1617.95, 1352.08, 1090.21, 890.51, 563.88, 437.95 cm^{-1}. HR-MS (+): *m*/*z* calcd for $C_{11}H_{23}Cl_2N_5O_8Pt + H^+$ $[M + H]^+$ 619.0644, found 620.0634. El. Anal. Calcd. for $C_{11}H_{23}Cl_2N_5O_8Pt$: % C = 21.33; H = 3.74; N = 11.31; found: % C = 21.64; H = 3.82; N = 11.72.

***N*-[2-*O*-(*β*-D-glucopyranosyl)-ethyl-1,2,3-triazol-4-yl)]-propanoic acid (21)**

Compound **21** was synthesised according to the procedure used for compound 11 (Yield 0.053 g, 0.152 mmol, 89%). R_f = 0.56 (DCM:MeOH:H_2O 60:35:5). $[\alpha]_D^{24.4}$+4.18 (c 0.716, MeOH). ^{1}H NMR (500 MHz, D_2O) δ 7.80 (s, 1H, triaz-C*H*), 4.57 (dd, *J* = 14.3, 3.5 Hz, 2H, CH_2-triaz), 4.35 (d, *J* = 6.8 Hz, 1H, H-1), 4.27–4.20 (m, 1H, OC*H*), 4.05 (dt, *J* = 6.2, 4.1 Hz, 1H, OC*H*′), 3.84 (d, *J* = 12.3 Hz, 1H, H-6), 3.67–3.60 (m, 1H, H-6′), 3.43–3.27 (m, 3H, H-3, H-4, H-5), 3.21–3.18 (m, 5H, H-2), 2.92 (td, *J* = 7.3, 1.3 Hz, 2H, triaz-CH_2), 2.53 (t, *J* = 7.4 Hz, 2H, CH_2CO). ^{13}C NMR (125 MHz, D_2O) δ 180.75 (*C*O), 147.40 (triaz-*C*), 123.72 (triaz-*C*H), 102.38 (C-1), 75.87 (C-3), 75.55 (C-5), 72.89 (C-2), 69.51 (C-4), 68.09 (OCH_2),

60.65 (C-6), 50.11 (CH_2-triaz), 36.01 (CH_2CO), 21.38 (triaz-CH_2). IR (ATR) 3334.48, 2885.68, 1711.54, 1553.96, 1358.20, 1219.58, 1030.84, 828.66, 494.93 cm^{-1}. HR-MS (+): m/z calcd for $C_{13}H_{21}N_3O_8$ + H^+ $[M + H]^+$ 348.1407, found 348.1402. HR-MS (+): m/z calcd for $C_{13}H_{21}N_3O_8$ + Na^+ $[M + Na]^+$ 370.1226, found 370.1218.

_N_-[2-_O_-(β-D-glucopyranosyl)-ethyl-1,2,3-triazol-4-yl)]-(3-oxopropyl-(oxy(2,5-dioxopyrrolidin-1-yl))) (23)

Compound **23** was synthesised according to the procedure for compound 13. (Yield 0.380 g, 0.855 mmol, 80%). R_f = 0.86 (DCM:MeOH:H_2O 60:35:5). $[\alpha]_D^{23.2}$+ 1.07 (c 0.93, MeOH). ^{1}H NMR (500 MHz, DMSO) δ 7.99 (s, 1H, triaz-C*H*), 5.10 (d, *J* = 5.0 Hz, 1H, O*H* of C-2), 4.99 (d, *J* = 4.8 Hz, 1H, O*H* of C-3), 4.94 (d, *J* = 5.3 Hz, 1H, O*H* of C-4), 4.52 (dt, *J* = 6.8, 4.2 Hz, 3H, CH_2-triaz, O*H* of C-6), 4.21 (d, *J* = 7.8 Hz, 1H, H-1), 4.06 (ddd, *J* = 10.6, 5.9, 4.4 Hz, 1H, OC*H*), 3.86 (ddd, *J* = 11.2, 6.7, 4.4 Hz, 1H, OC*H*′), 3.67 (ddd, *J* = 11.5, 5.9, 1.8 Hz, 1H, H-6), 3.43 (dt, *J* = 11.7, 5.9 Hz, 1H, H-6′), 3.16–3.08 (m, 2H, H-3, H-5), 3.08–3.01 (m, 3H, CH_2CO, H-4), 3.00–2.93 (m, 3H, H-2, triaz-CH_2), 2.81 (s, 4H, CH_2CH_2-succ). ^{13}C NMR (125 MHz, DMSO) δ 170.20 (*C*O succ x2), 168.33 (*C*O), 144.17 (triaz-*C*), 123.18 (triaz-*C*H), 102.86 (C-1), 76.97 (C-3), 76.57 (C-5), 73.31 (C-2), 70.01 (C-4), 67.31 (OCH_2), 61.08 (C-6), 49.54 (CH_2-triaz), 29.81 (CH_2CO), 25.45 (CH_2CH_2-succ), 20.37 (triaz-CH_2). IR (ATR) 3369.66, 2886.72, 1728.66, 1366.57, 1206.12, 1033.96, 813.22, 645.50 cm^{-1}. HR-MS (+): m/z calcd for $C_{17}H_{24}N_4O_{10}$ + H^+ $[M + H]^+$ 445.1571, found 445.1561. HR-MS (+): m/z calcd for $C_{17}H_{24}N_4O_{10}$ + Na^+ $[M + Na]^+$ 467.1390, found 467.1384.

$[Pt^{IV}(NH_3)_2$(21)$(OH)Cl_2]$ (3)

Complex **3** prepared according to the method reported for complex 1. (Yield 0.218 g, 0.328 mmol, 47%). $[\alpha]_D^{21.8}$+ 15 (c 0.4, H_2O). ^{1}H NMR (500 MHz, DMSO) δ 7.93 (s, 1H, triaz-C*H*), 5.98 (t, *J* = 48.2 Hz, 6H, 2x NH_3), 5.10 (d, *J* = 4.9 Hz, 1H, O*H* of C-2), 4.98 (d, *J* = 4.7 Hz, 1H, O*H* of C-3), 4.93 (d, *J* = 5.2 Hz, 1H, O*H* of C-4), 4.57–4.46 (m, 3H, CH_2-triaz, O*H* of C-6), 4.21 (d, *J* = 7.8 Hz, 1H, H-1), 4.10–4.03 (m, 1H, OC*H*), 3.89–3.83 (m, 1H, OC*H*′), 3.67 (dd, *J* = 10.7, 4.4 Hz, 1H, H-6), 3.43 (dd, *J* = 11.4, 5.6 Hz, 1H, H-6′), 3.16–3.09 (m, 2H, H-3, H-5), 3.03 (dd, *J* = 9.0, 4.0 Hz, 1H, H-4), 2.98–2.93 (m, 1H, H-2), 2.80 (t, *J* = 7.2 Hz, 2H, triaz-CH_2), 2.46 (d, *J* = 7.3 Hz, 2H, CH_2CO). ^{13}C NMR (125 MHz, DMSO) δ 179.94 (*C*O), 146.18 (triaz-*C*), 122.90 (triaz-*C*H), 102.82 (C-1), 76.95 (C-3), 76.54 (C-5), 73.32 (C-2), 69.99 (C-4), 67.27 (OCH_2), 61.06 (C-6), 49.42 (CH_2-triaz), 36.12 (CH_2CO), 22.01 (triaz-CH_2). ^{195}Pt{^{1}H} NMR (108 MHz, DMSO) δ 1047.34 ppm. IR (ATR) 3247.15, 1623.71, 1356.54, 1035.26, 578.92, 426.46 cm^{-1}. HR-MS (+): m/z calcd for $C_{13}H_{27}Cl_2N_5O_9Pt$ + H^+ $[M + H]^+$ 663.0907, found 664.0904. El. Anal. Calcd. for $C_{13}H_{27}Cl_2N_5O_9Pt$: % C = 23.54; H = 4.10; N = 10.56; found: % C = 23.27; H = 4.91; N = 10.11.

_N_-[2-_O_-(β-D-galactopyranosyl)-ethyl-1,2,3-triazol-4-yl)]-propanoic acid (22)

Compound **22** was prepared according to the procedure reported for compound 11 (Yield 0.231 g, 0.665 mmol, 96%). R_f = 0.30 (DCM:MeOH:H_2O 60:35:5). $[\alpha]_D^{23.2}$+ 4.24 (c 0.707, MeOH). ^{1}H NMR (500 MHz, D_2O) δ 7.85 (s, 1H, triaz-C*H*), 4.61 (t, *J* = 5.1 Hz, 2H, CH_2-triaz), 4.31 (d, *J* = 7.9 Hz, 1H, H-1), 4.26 (dt, *J* = 11.5, 4.7 Hz, 1H, OC*H*), 4.09–4.04 (m, 1H, OC*H*′), 3.87 (d, *J* = 3.4 Hz, 1H, H-4), 3.75–3.67 (m, 2H, H-6, H-6′), 3.62 (dd, *J* = 7.7, 4.6 Hz, 1H, H-5), 3.58 (dd, *J* = 9.9, 3.5 Hz, 1H, H-3), 3.45 (dd, *J* = 9.9, 7.9 Hz, 1H, H-2), 2.96 (t, *J* = 7.3 Hz, 2H, triaz-CH_2), 2.65 (t, *J* = 7.3 Hz, 2H, CH_2CO). ^{13}C NMR (125 MHz, D_2O) δ 178.90 (*C*O), 146.93 (*C*-triaz), 123.87 (*C*H-triaz), 102.97 (C-1), 75.08 (C-5), 72.58 (C-3), 70.55 (C-2), 68.53 (C-4), 68.02 (OCH_2), 60.87 (C-6), 50.19 (CH_2-triaz), 34.49 (CH_2CO), 20.72 (triaz-CH_2). IR (ATR) 3282.63, 2926.54, 1568.45, 1398.02, 1044.17, 781.51, 533.03 cm^{-1}. HR-MS (+): m/z calcd for $C_{13}H_{21}N_3O_8$ + H^+ $[M + H]^+$ 348.1407, found 348.1403. HR-MS (+): m/z calcd for $C_{13}H_{21}N_3O_8$ + Na^+ $[M + Na]^+$ 370.1226, found 370.1221.

_N_-[2-_O_-(β-D-galactopyranosyl)-ethyl-1,2,3-triazol-4-yl)]-(3-oxopropyl-(oxy(2,5-dioxopyrrolidin-1-yl))) (24)

Compound **24** was prepared according to the procedure reported for compound 13 (Yield 0.360 g, 0.810 mmol, 75%). R_f = 0.84 (DCM:MeOH:H_2O 60:35:5). $[\alpha]_D^{22.8}$+ 5.5 (c 0.366,

MeOH). ^{1}H NMR (500 MHz, DMSO) δ 7.99 (s, 1H, triaz-C*H*), 4.95 (d, *J* = 4.6 Hz, 1H, O*H* of C-2), 4.76 (d, *J* = 5.3 Hz, 1H, O*H* of C-3), 4.59 (t, *J* = 5.7 Hz, 1H, O*H* of C-6), 4.51 (qdd, *J* = 14.3, 6.4, 4.2 Hz, 2H, CH_2-triaz), 4.39 (d, *J* = 4.6 Hz, 1H, O*H* of C-4), 4.15 (d, *J* = 7.3 Hz, 1H, H-1), 4.05 (ddd, *J* = 10.7, 6.2, 4.3 Hz, 1H, OC*H*), 3.83 (ddd, *J* = 11.1, 6.7, 4.3 Hz, 1H, OC*H*′), 3.63–3.60 (m, 1H, H-4), 3.55–3.44 (m, 2H, H-6, H-6′), 3.34–3.24 (m, 3H, H-2, H-5, H-3), 3.07–3.03 (m, 2H, CH_2CO), 3.00–2.95 (m, 2H, triaz-CH_2), 2.81 (s, 4H, CH_2CH_2-succ). ^{13}C NMR (125 MHz, DMSO) δ 170.22 (*C*O succ x2), 168.35 (*C*O), 144.19 (triaz-*C*), 123.16 (triaz-CH), 103.48 (C-1), 75.37 (C-5), 73.30 (C-3), 70.41 (C-2), 68.15 (C-4), 67.20 (OCH_2), 60.46 (C-6), 49.56 (CH_2-triaz), 29.82 (CH_2CO), 25.46 (CH_2CH_2-succ), 20.38 (triaz-CH_2). IR (ATR) 3378.02, 2939.53, 1728.86, 1366.45, 1206.01, 1046.41, 648.73 cm^{-1}. HR-MS (+): *m*/*z* calcd for $C_{17}H_{24}N_4O_{10}$ + H^+ [M + H]$^+$ 445.1571, found 445.1559. HR-MS (+): *m*/*z* calcd for $C_{17}H_{24}N_4O_{10}$ + Na^+ [M + Na]$^+$ 467.1390, found 467.1385.

[Pt^{IV}(NH$_3$)$_2$(22)(OH)Cl$_2$] (4)

Complex **4** was prepared according to the procedure reported for complex 1 (Yield 0.296 g, 0.446 mmol, 61%). $[\alpha]_D^{22.8}$+ 3.36 (c 0.9, H_2O). ^{1}H NMR (500 MHz, DMSO) δ 7.93 (s, 1H, triaz-C*H*), 5.98 (t, *J* = 48.4 Hz, 6H, 2× NH_3), 4.96 (d, *J* = 4.3 Hz, 1H, O*H* of C-3), 4.77 (d, *J* = 4.4 Hz, 1H, O*H* of C-2), 4.59 (d, *J* = 5.1 Hz, 1H, O*H* of C-6), 4.55–4.41 (m, 2H, CH_2-triaz), 4.40 (d, *J* = 4.4 Hz, 1H, OH of C-4), 4.15 (d, *J* = 7.1 Hz, 1H, H-1), 4.05 (ddd, *J* = 14.4, 9.4, 6.4 Hz, 1H, OC*H*), 3.84 (ddd, *J* = 11.0, 6.5, 4.6 Hz, 1H, OC*H*′), 3.62 (s, 1H, H-4), 3.50 (dd, *J* = 12.2, 6.4 Hz, 2H, H-6, H-6′), 3.35 (s, 1H, H-5 overlaps with H_2O), 3.30–3.27 (m, 2H, H-2, H-3), 2.82–2.77 (m, 2H, triaz-CH_2), 2.46 (d, *J* = 7.3 Hz, 2H, CH_2CO). ^{13}C NMR (125 MHz, DMSO) δ 179.93 (*C*O), 146.19 (triaz-*C*), 122.88 (triaz-*C*H), 103.48 (C-1), 75.37 (C-5), 73.27 (C-3), 70.43 (C-2), 68.15 (C-4), 67.19 (OCH_2), 60.46 (C-6), 49.46 (CH_2-triaz), 36.12 (CH_2CO), 22.01 (triaz-CH_2). ^{195}Pt{^{1}H} NMR (108 MHz, DMSO) δ 1046.82 ppm. IR (ATR) 3215.30, 1618.19, 1358.28, 1061.49, 575.94 cm^{-1}. HR-MS (+): *m*/*z* calcd for $C_{13}H_{27}Cl_2N_5O_9Pt$ + H^+ [M + H]$^+$ 663.0907, found 664.0902. El. Anal. Calcd. for $C_{13}H_{27}Cl_2N_5O_9Pt$: % C = 23.54; H = 4.10; N = 10.56; found: % C = 23.18; H = 4.75; N = 10.06.

4. Conclusions

Four novel Pt(IV) pro-drugs, based on a cisplatin scaffold with carbohydrate vectors in axial positions, were synthetised, linking the sugar moiety and the metal centre via CuAAC click chemistry. These pro-drugs were functionalised with deprotected glyco-moieties that act as real vectors to selectively target cancer cells. Most of the carbohydrate-functionalised Pt-based complexes reported in literature contain protected acetylated sugars, due to an easy synthesis and purification procedure. The complexes were tested on a panel of two 2D and 3D OS (Osteosarcoma) cell lines, as well as on healthy OS cells. All the complexes showed very promising activity, comparable to the reference cisplatin, demonstrating that the presence of a monosaccharide does not hamper the anticancer effect. Notably, the complexes are much less active against the healthy line, showing a promising selectivity for these OS cell lines, with respect to cisplatin. The complexes were also particularly active in the 3D model, a more reliable system compared to 2D, with the most promising activity shown by complexes **2** and **4** with a galactose substituent. The role of galactose in the metabolism of cancer cells is attracting significant attention because of potential diagnostic and therapeutic possibilities [40,41]. While the role of the free sugars as targeting vectors is not completely confirmed, the selectivity shown in 2D studies is a solid base to hypothesise that the carbohydrate moieties play an important role in targeted therapies. More specific biological studies (beyond the scope of this work) should be conducted (i.e., inhibition of the GLUTs receptors), but this selectivity was not observed in the analogue protected-Pt(IV) pro-drugs, recently reported by us. While all the complexes showed very promising activity, the discrimination between the two linkers is not observed. These complexes have been conjugated to graphene oxide nanoparticles that act as delivering agents, to further enhance the selectivity. The next step in our studies is the synthesis and characterisation of analogous complexes, where the carbohydrate is conjugated via the C2 carbon (not the anomeric carbon) that was demonstrated to be the best in term of cellular recognition [42].

Supplementary Materials: The following supporting information can be downloaded at: https://www.mdpi.com/article/10.3390/ijms24076028/s1.

Author Contributions: Conceptualization, D.M., T.V.-T., M.M. and E.M.; methodology, D.M., E.M. and M.M.; formal analysis, E.M., G.B., A.R., E.C. and E.D.; investigation, E.M., G.B. and A.R.; curation, D.M., S.P. and M.M.; writing—original draft preparation, D.M., T.V.-T., E.M., M.M. and G.B.; supervision, D.M., T.V.-T. and M.M.; funding acquisition, D.M. and S.P. All authors have read and agreed to the published version of the manuscript.

Funding: This work was funded by the European Project Horizon 2020 NANO4TARMED (H2020-WIDESPREAD-2020-5; GA number 952063).

Data Availability Statement: The data presented in this study are available in the article and in the Supplementary Material.

Acknowledgments: E.M. is grateful to Maynooth University for sponsoring postgrad scholarship with a Graduate Teaching Fellowship. Science Foundation Ireland 2012 Strategic Opportunity Fund (Infrastructure award 12/RI/2346/SOF) for NMR facilities.

Conflicts of Interest: The authors declare that the research was conducted in the absence of any commercial or financial relationships that could be construed as a potential conflict of interest.

References

1. Mortensen, A.C.L.; Mohajershojai, T.; Hariri, M.; Pettersson, M.; Spiegelberg, D. Overcoming Limitations of Cisplatin Therapy by Additional Treatment With the HSP90 Inhibitor Onalespib. *Front. Oncol.* **2020**, *10*, 532285. [CrossRef] [PubMed]
2. Zhang, C.; Xu, C.; Gao, X.; Yao, Q. Platinum-based drugs for cancer therapy and anti-tumor strategies. *Theranostics* **2022**, *12*, 2115–2132. [CrossRef] [PubMed]
3. Kenny, R.G.; Marmion, C.J. Toward Multi-Targeted Platinum and Ruthenium Drugs—A New Paradigm in Cancer Drug Treatment Regimens? *Chem. Rev.* **2019**, *119*, 1058–1137. [CrossRef] [PubMed]
4. Fronik, P.; Gutmann, M.; Vician, P.; Stojanovic, M.; Kastner, A.; Heffeter, P.; Pirker, C.; Keppler, B.K.; Berger, W.; Kowol, C.R. A platinum(IV) prodrug strategy to overcome glutathione-based oxaliplatin resistance. *Commun. Chem.* **2022**, *5*, 46. [CrossRef] [PubMed]
5. Harrap, K.R.; Kelland, L.R.; Jones, M.; Goddard, P.M.; Orr, R.M.; Morgan, S.E.; Murrer, B.A.; Abrams, M.J.; Giandomenico, C.M.; Cobbleigh, T. Platinum coordination complexes which circumvent cisplatin resistance. *Adv. Enzym. Regul.* **1991**, *31*, 31–43. [CrossRef]
6. Bhargava, A.; Vaishampayan, U.N. Satraplatin: Leading the new generation of oral platinum agents. *Expert Opin. Investig. Drugs* **2009**, *18*, 1787–1797. [CrossRef]
7. Eastman, A. Glutathione-mediated activation of anticancer platinum(IV) complexes. *Biochem. Pharmacol.* **1987**, *36*, 4177–4178. [CrossRef]
8. Rischin, D.; Ling, V. Ormaplatin resistance is associated with decreased accumulation of its platinum (II) analogue, dichloro(D,L-trans)1,2-diaminocyclohexaneplatinum (II). *Br. J. Cancer* **1996**, *74*, 590–596. [CrossRef]
9. Pendyala, L.; Krishnan, B.S.; Walsh, J.R.; Arakali, A.V.; Cowens, J.W.; Creaven, P.J. Studies on the Human Metabolism of Iproplatin. *Cancer Chemother. Pharmacol.* **1989**, *25*, 10–14. [CrossRef]
10. Wheate, N.J.; Walker, S.; Craig, G.E.; Oun, R. The status of platinum anticancer drugs in the clinic and in clinical trials. *Dalton Trans.* **2010**, *39*, 8113–8127. [CrossRef]
11. Warburg, O.; Wind, F.; Negelein, E. The metabolism of tumors in the body. *J. Gen. Physiol.* **1927**, *8*, 519. [CrossRef] [PubMed]
12. Liu, C.; Jin, Y.; Fan, Z. The Mechanism of Warburg Effect-Induced Chemoresistance in Cancer. *Front. Oncol.* **2021**, *11*, 698023. [CrossRef] [PubMed]
13. Ma, L.; Ma, R.; Wang, Y.; Zhu, X.; Zhang, J.; Chan, H.C.; Chen, X.; Zhang, W.; Chiu, S.-K.; Zhu, G. Chalcoplatin, a dual-targeting and p53 activator-containing anticancer platinum(iv) prodrug with unique mode of action. *Chem. Commun.* **2015**, *51*, 6301–6304. [CrossRef] [PubMed]
14. Ma, J.; Yang, X.; Hao, W.; Huang, Z.; Wang, X.; Wang, P.G. Mono-functionalized glycosylated platinum(IV) complexes possessed both pH and redox dual-responsive properties: Exhibited enhanced safety and preferentially accumulated in cancer cells in vitro and in vivo. *Eur. J. Med. Chem.* **2017**, *128*, 45–55. [CrossRef] [PubMed]
15. Ma, J.; Wang, Q.; Huang, Z.; Yang, X.; Nie, Q.; Hao, W.; Wang, P.G.; Wang, X. Glycosylated Platinum(IV) Complexes as Substrates for Glucose Transporters (GLUTs) and Organic Cation Transporters (OCTs) Exhibited Cancer Targeting and Human Serum Albumin Binding Properties for Drug Delivery. *J. Med. Chem.* **2017**, *60*, 5736–5748. [CrossRef]
16. Ma, J.; Wang, Q.; Yang, X.; Hao, W.; Huang, Z.; Zhang, J.; Wang, X.; Wang, P.G. Glycosylated platinum(iv) prodrugs demonstrated significant therapeutic efficacy in cancer cells and minimized side-effects. *Dalton Trans.* **2016**, *45*, 11830–11838. [CrossRef]
17. Ma, J.; Liu, H.; Xi, Z.; Hou, J.; Li, Y.; Niu, J.; Liu, T.; Bi, S.; Wang, X.; Wang, C.; et al. Protected and De-protected Platinum(IV) Glycoconjugates With GLUT1 and OCT2-Mediated Selective Cancer Targeting: Demonstrated Enhanced Transporter-Mediated Cytotoxic Properties in vitro and in vivo. *Front. Chem.* **2018**, *6*, 386. [CrossRef]
18. Wang, Q.; Huang, Z.; Ma, J.; Lu, X.; Zhang, L.; Wang, X.; Wang, P.G. Design, synthesis and biological evaluation of a novel series of glycosylated platinum(iv) complexes as antitumor agents. *Dalton Trans.* **2016**, *45*, 10366–10374. [CrossRef]

19. Heymann, M.-F.; Lézot, F.; Heymann, D. The contribution of immune infiltrates and the local microenvironment in the pathogenesis of osteosarcoma. *Cell. Immunol.* **2019**, *343*, 103711. [CrossRef]
20. Kansara, M.; Teng, M.W.; Smyth, M.J.; Thomas, D.M. Translational biology of osteosarcoma. *Nat. Rev. Cancer* **2014**, *14*, 722–735. [CrossRef]
21. Li, C.; Cai, J.; Ge, F.; Wang, G. TGM2 knockdown reverses cisplatin chemoresistance in osteosarcoma. *Int. J. Mol. Med.* **2018**, *42*, 1799–1808. [CrossRef] [PubMed]
22. Moynihan, E.; Bassi, G.; Ruffini, A.; Panseri, S.; Montesi, M.; Velasco-Torrijos, T.; Montagner, D. Click Pt(IV)-Carbohydrates Pro-Drugs for Treatment of Osteosarcoma. *Front. Chem.* **2021**, *9*, 795997. [CrossRef] [PubMed]
23. Upadhyaya, K.; Hamidullah, H.; Singh, K.; Arun, A.; Shukla, M.; Srivastava, N.; Ashraf, R.; Sharma, A.; Mahar, R.; Shukla, S.K.; et al. Identification of gallic acid based glycoconjugates as a novel tubulin polymerization inhibitors. *Org. Biomol. Chem.* **2015**, *14*, 1338–1358. [CrossRef] [PubMed]
24. Sun, L.; Zeng, X.; Yan, C.; Sun, X.; Gong, X.; Rao, Y.; Yan, N. Crystal structure of a bacterial homologue of glucose transporters GLUT1–4. *Nature* **2012**, *490*, 361–366. [CrossRef] [PubMed]
25. Deng, D.; Xu, C.; Sun, P.; Wu, J.; Yan, C.; Hu, M.; Yan, N. Crystal structure of the human glucose transporter GLUT1. *Nature* **2014**, *510*, 121–125. [CrossRef] [PubMed]
26. Holman, G.D. Structure, function and regulation of mammalian glucose transporters of the SLC2 family. *Pflug. Arch.-Eur. J. Physiol.* **2020**, *472*, 1155–1175. [CrossRef] [PubMed]
27. Malik, M.S.; Ahmed, S.A.; Althagafi, I.I.; Ansari, M.A.; Kamal, A. Application of triazoles as bioisosteres and linkers in the development of microtubule targeting agents. *RSC Med. Chem.* **2020**, *11*, 327–348. [CrossRef]
28. Liu, X.; Barth, M.; Cseh, K.; Kowol, C.R.; Jakupec, M.A.; Keppler, B.K.; Gibson, D.; Weigand, W. Oxoplatin-Based Pt(IV) Lipoate Complexes and Their Biological Activity. *Chem. Biodivers.* **2022**, *19*, e202200695. [CrossRef]
29. Chen, C.K.J.; Kappen, P.; Gibson, D.; Hambley, T.W. *trans*-Platinum(iv) pro-drugs that exhibit unusual resistance to reduction by endogenous reductants and blood serum but are rapidly activated inside cells:^{1}H NMR and XANES spectroscopy study. *Dalton Trans.* **2020**, *49*, 7722–7736. [CrossRef]
30. Visvader, J.E. Cells of origin in cancer. *Nature* **2011**, *469*, 314–322. [CrossRef]
31. Cifuentes, M.; García, M.A.; Arrabal, P.M.; Martínez, F.; Yañez, M.J.; Jara, N.; Weil, B.; Domínguez, D.; Medina, R.A.; Nualart, F. Insulin regulates GLUT1-mediated glucose transport in MG-63 human osteosarcoma cells. *J. Cell. Physiol.* **2011**, *226*, 1425–1432. [CrossRef]
32. Arponen, M.; Jalava, N.; Widjaja, N.; Ivaska, K.K. Glucose transporters GLUT1, GLUT3, and GLUT4 have different effects on osteoblast proliferation and metabolism. *Front. Physiol.* **2022**, *13*, 1035516. [CrossRef]
33. Horvath, P.; Aulner, N.; Bickle, M.; Davies, A.M.; Del Nery, E.; Ebner, D.; Montoya, M.C.; Östling, P.; Pietiäinen, V.; Price, L.S.; et al. Screening out irrelevant cell-based models of disease. *Nat. Rev. Drug Discov.* **2016**, *15*, 751–769. [CrossRef] [PubMed]
34. Edmondson, R.; Broglie, J.J.; Adcock, A.F.; Yang, L. Three-Dimensional Cell Culture Systems and Their Applications in Drug Discovery and Cell-Based Biosensors. *ASSAY Drug Dev. Technol.* **2014**, *12*, 207–218. [CrossRef]
35. Krishnakumar, G.S.; Gostynska, N.; Dapporto, M.; Campodoni, E.; Montesi, M.; Panseri, S.; Tampieri, A.; Kon, E.; Marcacci, M.; Sprio, S.; et al. Evaluation of different crosslinking agents on hybrid biomimetic collagen-hydroxyapatite composites for regenerative medicine. *Int. J. Biol. Macromol.* **2018**, *106*, 739–748. [CrossRef] [PubMed]
36. Bassi, G.; Panseri, S.; Dozio, S.M.; Sandri, M.; Campodoni, E.; Dapporto, M.; Sprio, S.; Tampieri, A.; Montesi, M. Scaffold-based 3D cellular models mimicking the heterogeneity of osteosarcoma stem cell niche. *Sci. Rep.* **2020**, *10*, 22294. [CrossRef] [PubMed]
37. Dozio, S.M.; Montesi, M.; Campodoni, E.; Sandri, M.; Piattelli, A.; Tampieri, A.; Panseri, S. Differences in osteogenic induction of human mesenchymal stem cells between a tailored 3D hybrid scaffold and a 2D standard culture. *J. Mater. Sci. Mater. Med.* **2019**, *30*, 136. [CrossRef]
38. Dhara, S.C. A Rapid Method for the Synthesis of Cis-[$Pt(NH_3)_2Cl_2$]. *Indian J. Chem.* **1970**, *8*, 193–194.
39. Brandon, R.J.; Dabrowiak, J.C. Synthesis, characterization, and properties, of a group of platinum(IV) complexes. *J. Med. Chem.* **1984**, *27*, 861–865. [CrossRef]
40. Valle, S.; Alcalá, S.; Martin-Hijano, L.; Cabezas-Sáinz, P.; Navarro, D.; Muñoz, E.R.; Yuste, L.; Tiwary, K.; Walter, K.; Ruiz-Cañas, L.; et al. Exploiting oxidative phosphorylation to promote the stem and immunoevasive properties of pancreatic cancer stem cells. *Nat. Commun.* **2020**, *11*, 5265. [CrossRef]
41. Zheng, D.; Sussman, J.H.; Jeon, M.P.; Parrish, S.T.; MacMullan, M.A.; Delfarah, A.; Graham, N.A. AKT but not MYC promotes reactive oxygen species-mediated cell death in oxidative culture. *J. Cell Sci.* **2020**, *133*, jcs239277. [CrossRef] [PubMed]
42. Patra, M.; Awuah, S.G.; Lippard, S.J. Chemical Approach to Positional Isomers of Glucose–Platinum Conjugates Reveals Specific Cancer Targeting through Glucose-Transporter-Mediated Uptake in Vitro and in Vivo. *J. Am. Chem. Soc.* **2016**, *138*, 12541–12551. [CrossRef] [PubMed]